PHYSICAL REVIEW E **66**, 036202 (2002)

Chaotic dynamics and orbit stability in the parabolic oval billiard

V. Lopac

Division of Physics, Faculty of Chemical Engineering and Technology, University of Zagreb, Zagreb, Croatia

I. Mrkonjić and D. Radić

Department of Physics, Faculty of Sciences, University of Zagreb, Zagreb, Croatia

(Received 8 January 2002; published 10 September 2002)

Chaotic properties of the one-parameter family of oval billiards with parabolic boundaries are investigated. Classical dynamics of such billiard is mixed and depends sensitively on the value of the shape parameter. Deviation matrices of some low period orbits are analyzed. Special attention is paid to the stability of orbits bouncing at the singular joining points of the parabolic arcs, where the boundary curvature is discontinuous. The existence of such orbits is connected with the segmentation of the phase space into two or more chaotic components. The obtained results are illustrated by numerical calculations of the Poincaré sections and compared with the properties of the elliptical stadium billiards.

DOI: 10.1103/PhysRevE.66.036202 PACS number(s): 05.45.Ac

I. INTRODUCTION

Billiard is a dynamical system in which a point particle moves freely within a bounded domain, changing its direction by elastic specular collisions with the billiard walls. Two-dimensional billiards, as paradigmatic examples of chaos in Hamiltonian systems, have been extensively investigated during past decades. Among planar billiards without additional forces only the elliptical shape (including the circle) is integrable [1], whereas the rectangular billiards, in spite of the regular type of dynamics, exhibit many complicated properties in dependence on the side ratio [2,3]. The same is true for a broad class of polygonal billiards that are considered pseudointegrable [4–6]. The growing interest for billiards started when two ergodic billiards were discovered, the Sinai billiard [7] and the Bunimovich stadium billiard [8], with the walls consisting partly of straight segments and partly of circular arcs. Subsequent investigations have been concentrated around the criterion of exponential divergence and the focusing properties of the billiard arcs, with the aim to discover possible new ergodic billiards [9–11]. Contemporary investigations of classical billiards are mostly based on the fact that the planar billiards are only exceptionally integrable or fully chaotic and that the generic case has mixed dynamics. Such billiards may have the parameter-dependent boundaries with smoothly varying properties obeying the Kolmogorov-Arnold-Moser (KAM) theorem, but there are also billiards with singularities in the boundary [12–22]. These are reflected in the Poincaré diagrams as bifurcations with singular properties and through the segmentation of the chaotic fraction of the phase space into two or more chaotic subdomains. In these investigations the criteria of linear stability [1] are used to reveal the dynamical properties of regular and chaotic orbits. The billiards have also been important in the semiclassical and quantum physics, since the semiclassical limit and quantal properties are greatly influenced by the complicated dynamics of the classical system [23–27].

In this paper we introduce a symmetrical billiard with parabolic arcs, which we call the parabolic oval billiard. In Sec. II we describe the billiard and explain its geometrical properties. In Sec. III we analyze the stability and properties of some selected orbits and show the Poincaré diagrams depending on the shape parameter. In Sec. IV we discuss the segmentation of the chaotic part of the phase plane and compare the results with the properties of the elliptical stadium billiards. Sec. V contains the discussion and conclusions.

II. DESCRIPTION OF THE PARABOLIC OVAL BILLIARDS

The boundaries of the billiard we investigate depend on the shape parameter δ, and are described in the x-y plane by the expression

$$y=\pm\left[\delta+\frac{\delta^2-x^2}{4(1-\delta)}\right] \quad \text{if} \quad 0<|x|\leqslant\delta,$$

$$y=\pm\,\delta\sqrt{\frac{1-|x|}{1-\delta}} \quad \text{if} \quad \delta\leqslant|x|<1, \tag{1}$$

where $x\in[-1,1]$ and $0<\delta<1$.

The billiards (1) are shown in Fig. 1 for several values of the shape parameter δ. At the points $P(\pm\delta,\pm\delta)$ where the two arcs meet both the boundary curve and the tangent slope are continuous. The second derivative of the boundary, however, is discontinuous and leads to the curvature radius:

$$R=\frac{[4(1-\delta)^2+x^2]^{3/2}}{4(1-\delta)^2} \quad \text{if} \quad 0<|x|\leqslant\delta,$$

$$R=\frac{[4(1-\delta)(1-|x|)+\delta^2]^{3/2}}{2\,\delta(1-\delta)} \quad \text{if} \quad \delta\leqslant|x|<1. \tag{2}$$

The horizontal diameter of the billiard has the length 2, and the vertical diameter is $2H$, with

$$H=\frac{\delta(4-3\,\delta)}{4(1-\delta)}. \tag{3}$$

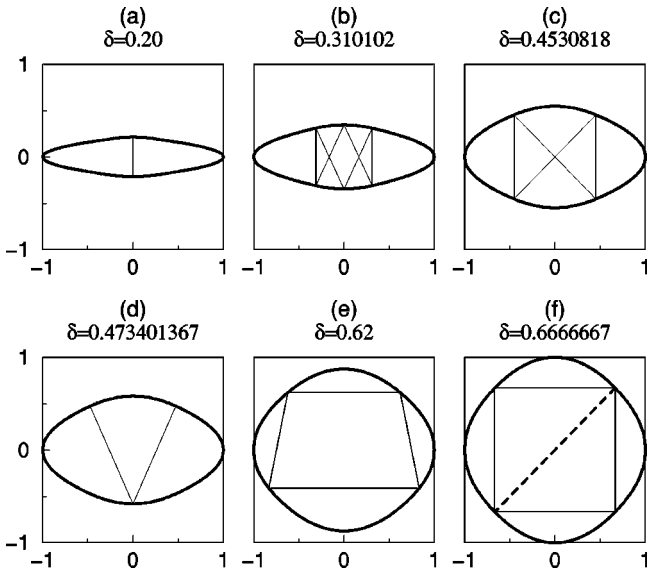

FIG. 1. The shape of the boundary (full line) of the parabolic oval billiard with some periodic orbits (thin line): (a) $\delta=0.20$, with the vertical two-bounce orbit; (b) $\delta=0.310\,102$, with the ''candy-shaped'' orbit; (c) $\delta=0.453\,081\,8$, with the ''bow-tie'' orbit; (d) $\delta=0.473\,401\,367$, with the ''bird'' orbit; (e) $\delta=0.62$, with the trapezoidal orbit; (f) $\delta=0.666\,666\,7$, with the four-period quadratic and the tilted two-bounce orbits.

For $\delta\to 0$ and $\delta\to 1$ the billiards are infinitely elongated ovals, and for $\delta=2/3$ the shape has the central symmetry. The coordinates of the focal points of the parabolas are

$$F_y(0,\pm[\delta+g(\delta)]),$$

$$F_x(\pm[\delta-g(\delta)],0), \tag{4}$$

with

$$g(\delta)=\frac{(3\delta-2)(2-\delta)}{4(1-\delta)}. \tag{5}$$

For $\delta<2/3$ the billiard is oriented horizontally (the vertical diameter is smaller than 2), and for $\delta>2/3$ it is elongated in the vertical direction. There exists a correspondence of the shapes when

$$\delta\to\frac{4-4\delta}{4-3\delta}. \tag{6}$$

Therefore, we show results only for the shapes $\delta\leqslant 2/3$, indicating where convenient the corresponding value $\delta>2/3$.

III. DYNAMICS OF THE PARTICLE IN THE PARABOLIC OVAL BILLIARD

When the shape parameter is varied, the properties of the parabolic oval billiard drastically change. Figure 2 shows the Poincaré sections for different shapes. As explained in [22], these diagrams are area conserving and are obtained by plotting the coordinate x and the x component v_x of the velocity of the particle at the moment when it crosses the x axis. In Figs. 2(c), 2(e), and 2(g), some singularities in the phase plane are observed which can be traced to special periodic orbits with the singular points on the boundary as the bouncing points.

Some typical orbits are shown in Fig. 1. The vertical diametral orbit is shown in Fig. 1(a). It is stable and exists for all values $\delta<(10-2\sqrt{3})/11=0.594\,172\,58$. For this value the orbit is neutral. After this value the vertical orbit disappears, and the tilted two-bounce orbit is born. (Equivalently, for $\delta>2/3$, there exists a stable horizontal two-bounce orbit for $\delta>\sqrt{3}-1=0.732\,050\,8$, and for smaller values of δ there is a stable tilted two-bounce orbit.)

Next we explore the low period periodic orbits that bounce at the singular points $P(\pm\delta,\pm\delta)$ in the boundary. Due to the different curvature radii R_l and R_r at the singular points, the traces $|\mathrm{Tr}\mathbf{M}|$ of the deviation matrix [1] have different values, depending on the direction (left, right) of approaching the singular point $P(\delta,\delta)$. The six-period ''candy'' orbit, shown in Fig. 1(b), which appears at $\delta=0.310\,102$, has the absolute value of the trace of the stability matrix equal to 2 if approached from one side, and smaller than 2 when approached from the other side. The same is true for the four-period ''bow-tie'' orbit shown in Fig. 1(c), appearing at $\delta=0.453\,081\,8$. Thus, here we have stable/neutral orbits, able to generate elliptic islands in the Poincaré sections. There is, however, a conspicuous asymmetry in this picture, as can be discerned from the Poincaré sections for $\delta=0.310\,102$ and $\delta=0.453\,081\,8$ shown in Figs. 2(c) and 2(e), respectively. The orbit of the ''bird'' type appearing at $\delta=0.473\,401\,367$ [Fig. 1(d)] has the traces from both directions larger than 2, and is therefore unstable. Its Poincaré section is shown in Fig. 2(g). Some details on these orbits are listed in Table I.

Figure 1(e) shows the trapezoidal orbit, which is typical of the parabolic arcs and has been present also in the parabolic lemon-shaped billiard [18]. Here, this orbit has the horizontal orientation, and exists for the horizontally elongated parabolic oval billiards ($\delta<2/3$). These trapezoidal orbits are neutral, and form the series of isolated points in the Poincaré diagrams, as can be noticed in Fig. 2(j). The limiting values of the lower and upper trapeze basis are $y_-=\mp\delta$ and $y_+=\pm\delta^3/[4(1-\delta)^2]$. The equivalent vertically oriented trapezoidal orbits exist for $\delta>2/3$. These orbits pass through the focal points (4). For the symmetrical billiard shape $\delta=2/3$ the trapezoidal orbit degenerates into the quadratic neutral orbit [Fig. 1(f)]. For the same shape there exists a neutral tilted two-bounce orbit. The Poincaré section corresponding to this symmetrical shape is shown in Fig. 2(k). Figure 2(l) gives an example of the Poincaré section for the vertically elongated ovals $\delta>2/3$, in this case equivalent to the horizontal shape depicted in Fig. 2(i).

The consequences of the singular ''candy-shaped'' orbit are more closely inspected in Fig. 3. In Fig. 3(a) the enlarged part of the Poincaré section from Fig. 2(c) is shown. There exists clearly the invariant curve separating the two regions in the phase plane. The elliptic island seen on this figure is due to the six-period N orbit shown in Fig. 3(b). Figure 3(c)

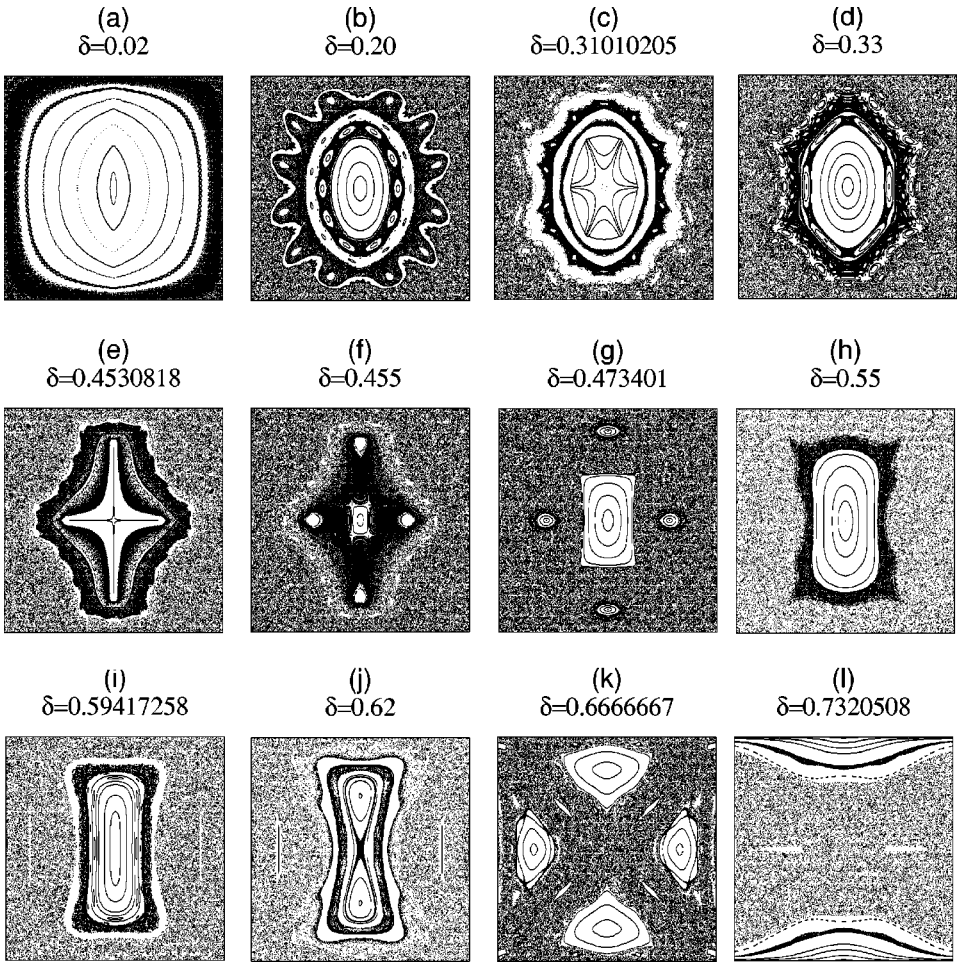

FIG. 2. Poincaré sections for the parabolic oval billiard. The position x and x component of the velocity v_x of the particle when crossing the x axis are shown. The range on both axes is $[-1,1]$. (a) $\delta=0.02$; (b) $\delta=0.2$; (c) $\delta=0.310\,102\,05$; (d) $\delta=0.33$; (e) $\delta=0.453\,081\,8$; (f) $\delta=0.455$; (g) $\delta=0.473\,401$; (h) $\delta=0.55$; (i) $\delta=0.594\,172\,58$; (j) $\delta=0.62$; (k) $\delta=0.666\,666\,7$; (l) $\delta=0.732\,050\,8$.

shows in more detail another region of the Poincaré section for $\delta=0.310\,102$. It zooms in on the point singularity corresponding to the six-period "candy-shaped" orbit seen in Fig. 1(b). As soon as δ increases above this value, the N orbit disappears and gives birth to stable elliptic islands corresponding to the six "candy-shaped" orbit, which can be observed in Fig. 2(d).

IV. SINGULAR PROPERTIES OF THE PARABOLIC OVAL BILLIARD AND COMPARISON WITH THE ELLIPTICAL STADIUM BILLIARD

The results presented in Sec. III reveal the important effects of the singular boundary points on the billiard dynamics. The calculated Poincaré diagrams show that for almost

TABLE I. Properties of some singular orbits in the parabolic oval billiards.

Orbit	Period	$\delta\leqslant 2/3$	Direction of approach	Tr**M**	Stability	Equivalent value $\delta\geqslant 2/3$
Tilted two-bounce	2	2/3 $=0.666\,666\,7$	l,r	2	Neutral	2/3 $=0.666\,666\,7$
Quadratic	4	2/3 $=0.666\,666\,7$	l,r	2	Neutral	2/3 $=0.666\,666\,7$
"Bird"	4	$(2/15)(6-\sqrt{6})$ $=0.473\,401\,367$	l r	2.57 4.28	Unstable Unstable	$\sqrt{(2/3)}$ $=0.816\,497$
"Bow-tie"	4	$(6-2\sqrt{2})/7$ $=0.453\,081\,8$	l r	2 1.88	Neutral Stable	$2(\sqrt{2}-1)$ $=0.828\,427$ ("Hour-glass")
"Candy"	6	$(4-\sqrt{6})/5$ $=0.310\,102$	l r	−0.33 2	Stable Neutral	$2\sqrt{6}-4$ $=0.898\,979$

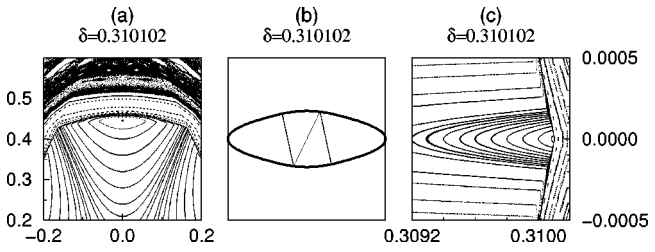

FIG. 3. Strongly magnified part of the Poincaré section for $\delta = 0.310\,102$ containing the elliptical invariant point and the invariant curve separating the two domains; (b) the *N*-orbit responsible for the elliptic point shown in (a); (c) strongly magnified part of the Poincaré section for $\delta = 0.310\,102$ containing the point corresponding to the ''candy-shaped'' orbit.

all values of δ the phase space is divided into separate domains which do not overlap. This is verified by numerical calculations up to 10^7 bounces. For special irrational parameter values corresponding to the orbits bouncing at the singular points, there is a strong numerical indication that there exist special closed invariant curves securing this separation. However, the segmentation is present also for other parameter values. The orbits become sticky and do not leave their areas within the phase plane.

Here it should be stressed that the billiard (1) can be considered as a special case of a larger family of billiards which arise when the two pairs of symmetrical arcs are appended at the vertices of the rectangle, in such a way that the tangent slope is continuous, and the curvature is discontinuous. The most familiar of such billiards is the Bunimovich stadium billiard [8] with straight segments connected by circular arcs. The next subfamily are the oval billiards of Benettin and Strelcyn [12], examined also by Hénon and Wisdom [14], who discovered in these billiards the existence of the separating invariant curves for some special types of singular orbits.

Furthermore, there is the two-parameter family of elliptical stadium billiards that were first introduced by Donnay [10] and which were also treated in Refs. [11,28–30]. We investigated systematically a broad shape range of this family of billiards [31]. We have found that the dynamics of this billiard is extremely rich, ranging from limiting integrable cases and simple mixed behavior obeying the KAM theorem, through the fully ergodic billiards for certain parameter ranges, to the mixed phase-space properties with strongly enhanced segmentation of the phase plane. In our analysis we used the parametrization of the shape of the elliptical stadium where the boundary is described as

$$y = \pm\gamma \quad \text{if} \quad 0 < |x| \leqslant \delta,$$

$$y = \pm\gamma\sqrt{1-\left(\frac{|x|-\delta}{1-\delta}\right)^2} \quad \text{if} \quad \delta \leqslant |x| < 1, \tag{7}$$

where $x \in [-1,1]$, $0 \leqslant \delta \leqslant 1$ and $0 < \gamma < \infty$. As stressed in Refs. [10,11], the possibility of ergodic behavior is present if the ratio of the two semiaxes is $1 \leqslant (1-\delta)/\gamma < \sqrt{2}$.

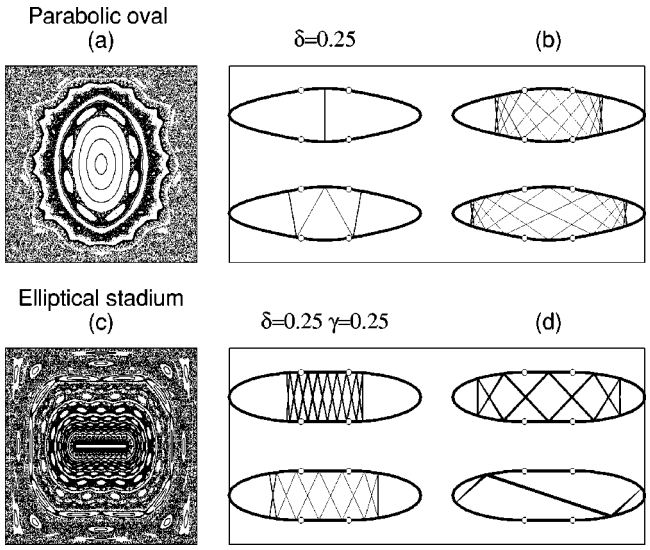

FIG. 4. (a) The Poincaré section for the parabolic oval billiard with $\delta = 0.25$. (b) Some typical orbits for the parabolic oval billiard presented in (a). (c) The Poincaré section for the elliptical stadium billiard with $\delta = 0.25$ and $\gamma = 0.25$. (d) Some typical orbits for the elliptical stadium billiard presented in (c).

Those shapes can be reduced to one-parameter families in many different ways. For instance, for $\gamma = 1 - \delta$ one obtains a family of Bunimovich stadium billiards. In all cases the horizontal diameter is equal to 2.

If $\delta = \gamma$, the straight segments and elliptic arcs meet at the vertices of a square of side 2δ, the same as in the parabolic oval billiard. In Fig. 4 we compare the Poincaré section [Fig. 4(a)] and some periodic orbits from different segments of the phase plane [Fig. 4(b)] for the parabolic oval billiard with the corresponding Poincaré section [Fig. 4(c)] and the orbits [Fig. 4(d)] for the elliptical stadium billiard. In the right upper angle of Fig. 4(d) one notices one of the orbits that were called pantografic in Ref. [29], and which are a generalization of the ''candy-shaped'' orbit. As is seen from Fig. 4(d), not only pantografic orbits, but also other types of orbits contribute significantly to the overall dynamics in the elliptical stadium billiard.

V. DISCUSSION AND CONCLUSIONS

In summarizing the results presented in the preceding sections, we can draw the following conclusions. The two-dimensional parabolic oval billiard introduced in this work offers a new possibility for exploring the effects of the discontinuities in the curvature radius on the structure of the phase space. We have calculated analytically the deviation matrices of the main lowest periodic orbits and performed extensive numerical calculations of the Poincaré sections. Our results show that for all values of the shape parameter the phase plane is segmented into separated domains with complex fractal structure. Properties of the parabolic oval billiard are in some details similar to those of the elliptical stadium billiard, but exhibit also significant differences. This confirms that the important modifications in the billiard dy-

namics are introduced when the curved boundary segments are replaced by straight lines.

In the light of the recent interest in exploring quantal repercussions of the classical chaos in the parameter-dependent mixed Hamiltonian systems [19,27,32,33], the parabolic oval billiard opens numerous possibilities for calculating the level density fluctuations, wave functions, and localization phenomena. The investigations in these directions are now in progress and hopefully will contribute farther to the understanding of complicated dynamics in the mixed systems that are out of reach of the KAM theorem.

ACKNOWLEDGMENTS

The authors wish to thank A. Bäcker, V. Dananić, H. Makino, T. Prosen, and M. Robnik for illuminating discussions.

[1] M. Berry, Eur. J. Phys. **2**, 91 (1981).
[2] M. Robnik and G. Veble, J. Phys. A **31**, 4669 (1998).
[3] R. Connors and J. Keating, J. Phys. A **31**, 4669 (1999).
[4] D. Biswas, Phys. Rev. E **54**, R1044 (1996).
[5] R. Artuso, G. Casati, and I. Guarneri, Phys. Rev. E **55**, 6384 (1997).
[6] G. Casati and T. Prosen, Phys. Rev. Lett. **83**, 4729 (1999).
[7] Y.G. Sinai, Russ. Math. Surveys **25**, 137 (1970).
[8] L. Bunimovich, Funct. Anal. Appl. **8**, 254 (1974).
[9] M. Wojtkowski, Commun. Math. Phys. **105**, 391 (1986).
[10] V. Donnay, Commun. Math. Phys. **141**, 225 (1991).
[11] R. Markarian, Nonlinearity **6**, 819 (1993).
[12] G. Benettin and J. Strelcyn, Phys. Rev. A **17**, 773 (1978).
[13] M. Robnik, J. Phys. A **16**, 3971 (1983).
[14] M. Hénon and J. Wisdom, Physica D **8**, 157 (1983).
[15] A. Bäcker, F. Steiner, and P. Stifter, Phys. Rev. E **52**, 2463 (1995).
[16] H. Dullin, P. Richter, and A. Wittek, Chaos **6**, 43 (1996).
[17] A. Bäcker and H. Dullin, J. Phys. A **30**, 1991 (1997).
[18] V. Lopac, I. Mrkonjić, and D. Radić, Phys. Rev. E **59**, 303 (1999).
[19] H. Makino, T. Harayama, and Y. Aizawa, Phys. Rev. E **59**, 4026 (1999).
[20] S. Ree and L. Reichl, Phys. Rev. E **60**, 1607 (1999).
[21] H. Makino, T. Harayama, and Y. Aizawa, Phys. Rev. E **63**, 056203 (2001).
[22] V. Lopac, I. Mrkonjić, and D. Radić, Phys. Rev. E **64**, 016214 (2001).
[23] S. McDonald and A. Kaufman, Phys. Rev. Lett. **42**, 1189 (1979).
[24] O. Bohigas, M. Giannoni, and C. Schmit, Phys. Rev. Lett. **52**, 1 (1984).
[25] E. Heller and S. Tomsovic, Phys. Today **46** (7), 38 (1993).
[26] T. Prosen and M. Robnik, J. Phys. A **27**, 8059 (1994).
[27] M. Robnik, Nonlin. Phenom. Complex Syst. **1**, 1 (1998).
[28] R. Markarian, S.O. Kamphorst, and S.P. de Carvalho, Commun. Math. Phys. **174**, 661 (1996).
[29] E. Canale, R. Markarian, S.O. Kamphorst, and S.P. de Carvalho, Physica D **115**, 189 (1998).
[30] S.O. Kamphorst and S.P. de Carvalho, Discrete Contin. Dyn. Syst., Ser. A **7**, 663 (2001).
[31] V. Lopac, I. Mrkonjić, and D. Radić (unpublished).
[32] M. Berry and M. Robnik, J. Phys. A **17**, 2413 (1984).
[33] J. Kole, K. Michielsen, and H.D. Raedt, Phys. Rev. E **63**, 016201 (2000).